Journal of Power Sources 201 (2012) 174–178

Contents lists available at SciVerse ScienceDirect

Journal of Power Sources

journal homepage: www.elsevier.com/locate/jpowsour

Short communication

Hydride reduced $LaSrCoO_{4-\delta}$ as new cathode material for $Ba(Zr_{0.1}Ce_{0.7}Y_{0.2})O_3$ based intermediate temperature solid oxide fuel cells

Bo Peng, Gang Chen*, Tao Wang, Jun Zhou, Jiaojiao Guo, Yonghong Cheng, Kai Wu

State Key Laboratory of Electrical Insulation and Power Equipment, Xi'an Jiaotong University, 28 Xianning West Road, Xi'an 710049, China

ARTICLE INFO

Article history:
Received 14 September 2011
Received in revised form 29 October 2011
Accepted 31 October 2011
Available online 6 November 2011

Keywords:
Intermediate temperature solid oxide fuel cell
Hydride reduced phase
Proton conducting electrolyte
Composite cathode
Electrochemical property

ABSTRACT

Cathodes with high catalytic activities are usually required for the preparation of high performance intermediate temperature (600–800 °C) solid oxide fuel cells (IT-SOFCs). In the present study, a new kind of cathode material for IT-SOFCs based on $Ba(Zr_{0.1}Ce_{0.7}Y_{0.2})O_3$ (BZCY) electrolytes is prepared through solid state reduction of the K_2NiF_4 structured $LaSrCoO_{4-\delta}$ with CaH_2. Structural analysis by XRD reveals that the cell parameters of $LaSrCoO_{4-\delta}$ become larger after the reduction. And oxygen stoichiometry of 3.57 is determined by iodometric titration for the CaH_2 reduced phase (marked as H-$LaSrCoO_{4-\delta}$). The electrochemical properties of both the H-$LaSrCoO_{4-\delta}$–BZCY and the $LaSrCoO_{4-\delta}$–BZCY composite cathodes are investigated through *ac* impedance spectroscopy and *dc* polarization measurements. At 750 °C, the H-$LaSrCoO_{4-\delta}$–BZCY cathode exhibits a polarization resistance of 0.229 Ω cm^2, which is about one third smaller than that of the $LaSrCoO_{4-\delta}$–BZCY cathode. Meanwhile, cathodic overpotential of 25 mV is obtained for the H-$LaSrCoO_{4-\delta}$–BZCY cathode under a current density of 100 mA cm^{-2} at 750 °C. This value is much lower than 70 mV of the $LaSrCoO_{4-\delta}$–BZCY cathode obtained at the same condition. Subsequent study on the cathodic reaction process implies that the better electrochemical properties of the H-$LaSrCoO_{4-\delta}$–BZCY cathode can be attributed to the higher oxygen vacancy concentration in the H-$LaSrCoO_{4-\delta}$ lattice that enhances some key steps of the oxygen reduction reaction (ORR).

1. Introduction

Solid oxide fuel cells (SOFCs) are considered as promising power generating devices for their obvious advantages like high energy efficiency, low environmental impact and excellent fuel flexibility. However, on their way to broad commercialization there are still some problems to be solved. For example, the high operating temperature (800–1000 °C) has limited the application of SOFCs for the high fabrication cost of expensive thermostable interconnectors and the compatibility problems between electrode and electrolyte materials. So the current trend is to develop SOFCs that operate in the intermediate temperature range (600–800 °C) [1]. However, both the electrolyte ionic conductivity and the cathode kinetics will inevitably decrease in this temperature range, resulting in dramatic degradation of the cell performance. For these reasons, considerable efforts have been made to find new electrolytes with higher ionic conductivity and suitable cathodes with better electrochemical properties [2–8].

Despite the widespread use of oxygen-ion conducting electrolytes like yttria stabilized zirconia (YSZ) and gadolinia doped ceria (GDC), proton conductors with higher conductivity at lower temperature have attracted more attention as new SOFC electrolytes in recent years. In 2006, Liu et al. successfully developed a novel proton conductor, $Ba(Zr_{0.1}Ce_{0.7}Y_{0.2})O_3$ (BZCY), which can be used as the electrolyte material of low temperature SOFCs. According to their study, BZCY shows both high proton conductivity and sufficient chemical and thermal stabilities at low temperatures [9]. And researches on cathode materials for BZCY based SOFCs are still under way.

Nowadays, K_2NiF_4-type oxides arouse intense interests for their potential application in SOFC cathodes. As compared with traditional perovskite structured materials, these oxides possess better thermal stability, higher surface oxygen exchange coefficients as well as closer thermal expansion coefficients to those of the commonly used SOFC electrolytes [10–12]. For oxides used as SOFC cathode materials, the presence of sufficient lattice oxygen vacancies is generally of positive influence on the oxygen reduction process [13,14]. Recently, some researchers reported a solid state reduction method utilizing metal hydrides as the reducing agents to achieve topologic oxide deintercalation and forming novel oxygen-deficient phases [15–17]. Although the magnetic properties of these phases were paid close attention, their electrochemical properties related to the use as SOFC cathode materials have not been studied.

* Corresponding author. Tel.: +86 029 82668493; fax: +86 029 82668493.
E-mail address: chainway@126.com (G. Chen).

0378-7753/$ – see front matter © 2011 Elsevier B.V. All rights reserved.
doi:10.1016/j.jpowsour.2011.10.121

In this paper, we first synthesized a highly oxygen-deficient phase through solid state reduction of the K_2NiF_4-type $LaSrCoO_{4-\delta}$ with CaH_2. Electrochemical properties of the reduced phase were then investigated to explore its potential use as cathode material for BZCY based IT-SOFCs.

2. Experimental

2.1. Preparation of cathode and electrolyte powders

$LaSrCoO_{4-\delta}$ powder was synthesized through the Pechini method [18]. Stoichiometric amounts of analytically pure $La(NO_3)_3{\cdot}6H_2O$, $Sr(NO_3)_2$ and $Co(NO_3)_3{\cdot}6H_2O$ were dissolved in a certain amount of deionized water. Citric acid, in a molar ratio of 4.5:1 to the total metallic ions, was subsequently added to obtain a homogeneous solution. Then, the solution was heated at 110 °C to form a porous gel. And $LaSrCoO_{4-\delta}$ black powder was finally obtained by calcining the gel at 1000 °C in air for 4 h. To get H-$LaSrCoO_{4-\delta}$, a mixture of $LaSrCoO_{4-\delta}$ and CaH_2, with a molar ratio of 2:1, was sealed in an evacuated silica tube under dynamic vacuum ($P \leq 2 \times 10^{-2}$ Pa) and heated at 450 °C for 24 h. The reaction products were filtrated with 0.1 M NH_4Cl solution in methanol to remove the CaO byproduct and any unreacted CaH_2 and then dried at 60 °C in an oven.

BZCY powder was prepared through the solid state reaction method. Appropriate amounts of high-purity $BaCO_3$, ZrO_2, CeO_2, and Y_2O_3 were uniformly mixed by ball milling in ethanol for 2 h. The mixture was then calcined at 1200 °C for 12 h to produce single phase BZCY.

2.2. Fabrication of cathodes

Three-electrode system was fabricated to test the electrochemical properties. First, electrolyte substrates were prepared by die pressing BZCY powder, followed by sintering at 1600 °C in air for 6 h. The electrolyte substrates were 17 mm in diameter and 1 mm in thickness. Then, the cathode slurry containing H-$LaSrCoO_{4-\delta}$ (or $LaSrCoO_{4-\delta}$) and BZCY (in a weight ratio of 7:3) was screen-printed onto one side of the BZCY electrolyte and calcined at 1100 °C for 3 h to form a 0.28 cm^2 working electrode. A Pt mesh counter electrode was placed symmetrically on the opposite side and a Pt mesh reference electrode was laid 3 mm away from the counter electrode, ensuring that this distance was at least three times the thickness of the electrolyte [19].

2.3. Characterization

For phase identification and chemical compatibility confirmation, powder X-ray diffraction (XRD) was performed on a Rigaku D/Max-2400 diffractometer (Cu Kα radiation, 40 kV, 100 mA, λ = 0.154178 nm) at a step of 0.02° and in a 2θ range of 20–70°. Rietveld refinements were performed to get information about the lattice structure. The average oxidation state of the cobalt ion and hence the oxygen stoichiometry of the original and reduced $LaSrCoO_{4-\delta}$ was determined by the iodometric titration technique [20]. And the microstructures of the composite cathodes were inspected by scanning electron microscopy (SEM) (JEOL JSM-6390).

Cathode polarization resistance (R_p) as a function of temperature and oxygen partial pressure (P_{O_2}) was characterized by *ac* impedance spectroscopy using Solartron 1287 potentiostat and 1260 frequency-response analyzer over a frequency range of 10^{-2}–10^5 Hz. Cathodic overpotential was obtained through *dc* polarization experiments which were taken at various potential steps by recording the current density as a function of time [21].

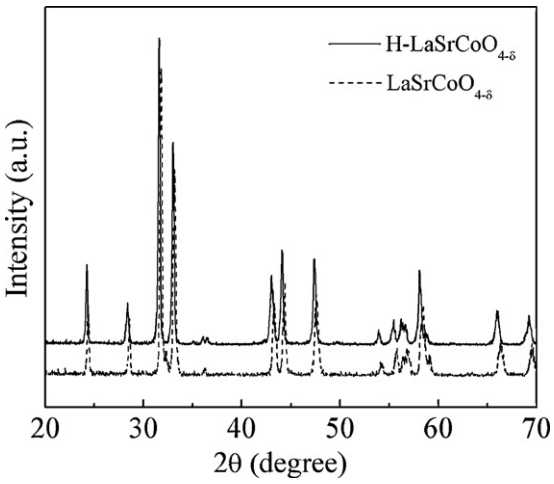

Fig. 1. XRD patterns of $LaSrCoO_{4-\delta}$ and H-$LaSrCoO_{4-\delta}$.

3. Results and discussions

3.1. Phase identification

Shown in Fig. 1 is a comparison of XRD patterns between $LaSrCoO_{4-\delta}$ and H-$LaSrCoO_{4-\delta}$. It can be confirmed that all the diffraction peaks of the two phases are characteristic of K_2NiF_4 structure with tetragonal symmetry. No obvious impurities are detected in H-$LaSrCoO_{4-\delta}$, indicating a complete remove of the unwanted phases through filtration by NH_4Cl solution. Furthermore, compared with the diffraction peaks of $LaSrCoO_{4-\delta}$, the corresponding peaks of H-$LaSrCoO_{4-\delta}$ shifted to the position of the smaller 2θ angles. This reflects the difference of cell parameters between the two phases. According to Hayward's report, during the reaction between $LaSrCoO_{4-\delta}$ and CaH_2, oxide ions were extracted from the $LaSrCoO_{4-\delta}$ lattice and reacted with CaH_2 to form CaO. And oxygen vacancies were simultaneously produced with the consumption of oxide ions [17]. The formation of oxygen vacancies led to the increase of Co–O bond length and caused changes in the unit cell parameters [22–25]. Table 1 lists the unit cell parameters of the two phases derived from Rietveld refinements. It is clear that the cell parameters became larger after $LaSrCoO_{4-\delta}$ was reduced. The oxygen stoichiometry of both $LaSrCoO_{4-\delta}$ and H-$LaSrCoO_{4-\delta}$ was later calculated with the iodometric titration results as 3.81 and 3.57, respectively. These data show that the reduced phase, H-$LaSrCoO_{4-\delta}$, has more oxygen vacancies.

3.2. Chemical compatibility

Reactions between cathodes and electrolytes generally introduce undesirable phases that may degrade the SOFC performance. To check the bulk chemical compatibility between H-$LaSrCoO_{4-\delta}$ and BZCY, a mixture of the two powders (in a 1:1 weight ratio) was calcined at 1100 °C for 3 h. Fig. 2 shows the XRD patterns of H-$LaSrCoO_{4-\delta}$, BZCY and their mixture after calcination. It is clear that both H-$LaSrCoO_{4-\delta}$ and BZCY remain their structures unchanged, implying no observable chemical reactions occurred between the two materials during the high temperature treatment.

Table 1
Comparison of unit cell parameters between H-$LaSrCoO_{4-\delta}$ and $LaSrCoO_{4-\delta}$.

Phase	Structure	*a* (Å)	*c* (Å)	*V* (Å^3)
H-$LaSrCoO_{4-\delta}$	Tetragonal	3.833	12.566	184.618
$LaSrCoO_{4-\delta}$	Tetragonal	3.807	12.452	180.470

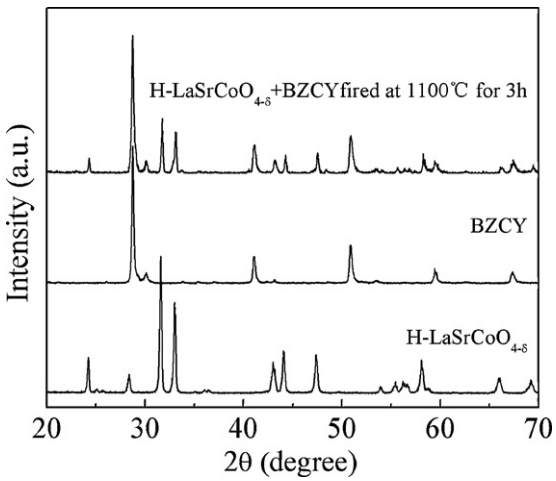

Fig. 2. XRD patterns of H-$LaSrCoO_{4-\delta}$, BZCY and H-$LaSrCoO_{4-\delta}$–BZCY mixture calcined at 1100 °C for 3 h.

So a preliminary conclusion can be drawn that H-$LaSrCoO_{4-\delta}$ is chemically compatible with the BZCY electrolyte.

3.3. Electrochemical properties of cathodes

Fig. 3 shows the polarization resistances of the H-$LaSrCoO_{4-\delta}$–BZCY and the $LaSrCoO_{4-\delta}$–BZCY cathodes at different temperatures. In addition to the smaller activation energy for the ORR, the H-$LaSrCoO_{4-\delta}$–BZCY cathode has the smaller polarization resistances at all temperatures. For example, the R_p value of the H-$LaSrCoO_{4-\delta}$–BZCY cathode is 0.229 Ω cm^2 at 750 °C, which is about one third decrease from 0.341 Ω cm^2 of the $LaSrCoO_{4-\delta}$–BZCY cathode.

To investigate the microstructure of the two cathodes, SEM images were taken from both their surfaces and cross-sections.

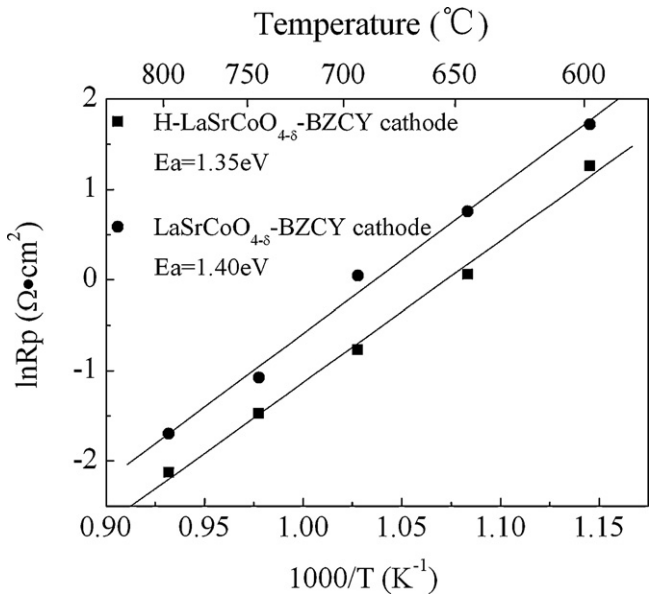

Fig. 3. Temperature dependence of the polarization resistance of the H-$LaSrCoO_{4-\delta}$–BZCY and the $LaSrCoO_{4-\delta}$–BZCY cathodes.

As can be seen in Fig. 4, both the H-$LaSrCoO_{4-\delta}$–BZCY and the $LaSrCoO_{4-\delta}$–BZCY cathodes exhibit good inter-particle connectivity and moderate pore structure. As the two cathodes have the similar microstructure, the difference between their electrochemical properties should be analyzed from the specific process of the oxygen reduction reaction. On the basis of other related researches [13], we can reasonably figure out the route of the ORR that occurs on the composite cathodes. The reduction process includes: (1) diffusion of gaseous oxygen through the porous cathode; (2) adsorption of oxygen molecules on H-$LaSrCoO_{4-\delta}$ (or $LaSrCoO_{4-\delta}$)

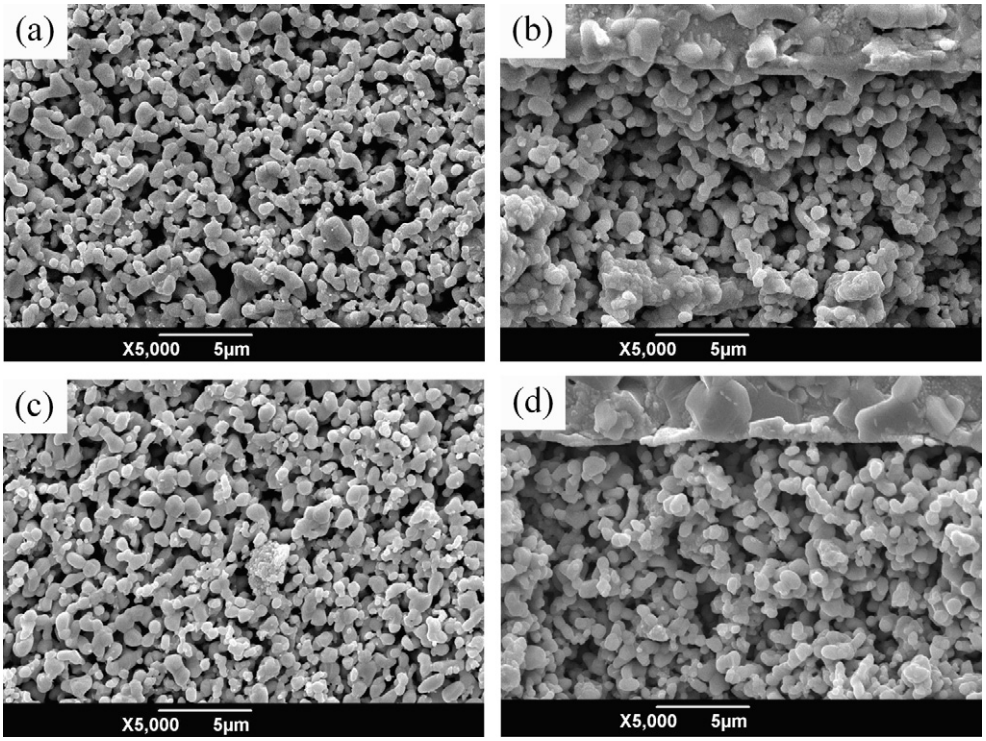

Fig. 4. Microstructures (SEM images) of cathodes fired at 1100 °C for 3 h: (a and b) surface and cross-section views of the H-$LaSrCoO_{4-\delta}$–BZCY cathode; (c and d) surface and cross-section views of the $LaSrCoO_{4-\delta}$–BZCY cathode.

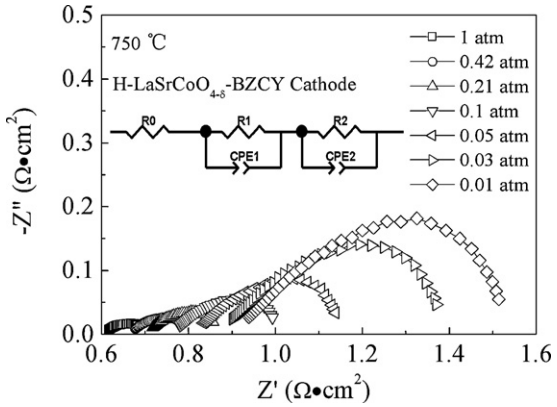

Fig. 5. Impedance spectra of the H-LaSrCoO$_{4-\delta}$–BZCY cathode under various oxygen partial pressures at 750 °C and the equivalent circuit for fitting the data.

surface; (3) dissociation of the adsorbed oxygen molecules into atoms; (4) reduction of oxygen atoms to oxide ions; (5) surface diffusion of oxide ions to the sites where H-LaSrCoO$_{4-\delta}$ (or LaSrCoO$_{4-\delta}$) and BZCY particles meet to combine with protons to form water molecules.

To confirm the rate-determining steps, P_{O_2} dependence of R_p for the two cathodes were investigated at different temperatures. Fig. 5 shows the typical impedance spectra of the H-LaSrCoO$_{4-\delta}$–BZCY cathode under various oxygen partial pressures at 750 °C. Two characteristics of the impedance spectra are readily noticeable. First, the impedance spectrum becomes larger with the decrease of P_{O_2}, indicating a gradually increasing polarization resistance and the great influence of oxygen concentration on the ORR process. Second, all the impedance spectra are composed of two overlapping arcs, implying the polarization resistance mainly comes from two rate-determining steps.

Here the equivalent circuit shown in Fig. 5 was employed to fit the impedance spectra. And the polarization resistances of the H-LaSrCoO$_{4-\delta}$–BZCY cathode were calculated from the fitting results. To make a comparison, the polarization resistances of the LaSrCoO$_{4-\delta}$–BZCY cathode were also calculated. The P_{O_2} dependence of R_p for the two cathodes is shown in Fig. 6. As we know, the relation between the polarization resistance and the oxygen partial pressure can be expressed as: $R_p = k(P_{O_2})^{-n}$, where k is the oxygen partial pressure independent constant. Different n values are attributed to different rate-determining steps [26]:

$n = 1$, diffusion of oxygen and adsorption of oxygen molecules on the cathode surface;
$n = 1/2$, dissociation of adsorbed oxygen molecules into atoms;
$n = 1/4$, charge transfer of oxygen atoms to become lattice oxide ions.

On one hand, the H-LaSrCoO$_{4-\delta}$–BZCY cathode shows n values between 1/4 and 1/2, implying dissociation and charge transfer are the rate-determining steps. On the other hand, the n value gets closer to 1/2 as the temperature increases, indicating the dissociation step makes the greater contribution to R_p at higher temperatures. Similar characteristics of n values were also found for the LaSrCoO$_{4-\delta}$–BZCY cathode. This suggests that there is no significant difference between the ORR mechanisms for the two cathodes. So, the smaller R_p value of the H-LaSrCoO$_{4-\delta}$–BZCY cathode shown in Fig. 3 can be explained from the perspective of the lattice structure. For the H-LaSrCoO$_{4-\delta}$–BZCY cathode, the higher oxygen vacancy concentration of the H-LaSrCoO$_{4-\delta}$ phase made the dissociation and the charge transfer steps easier to proceed than the corresponding steps of the ORR on the LaSrCoO$_{4-\delta}$–BZCY cathode [13]. This led to the smaller polarization resistance of the

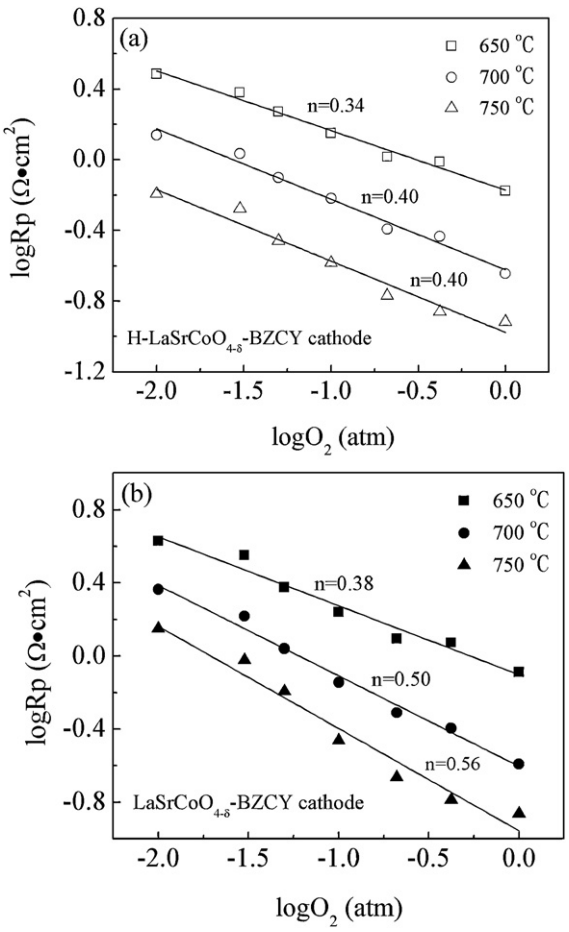

Fig. 6. Oxygen partial pressure dependence of the polarization resistance of (a) the H-LaSrCoO$_{4-\delta}$–BZCY and (b) the LaSrCoO$_{4-\delta}$–BZCY cathodes.

H-LaSrCoO$_{4-\delta}$–BZCY cathode than that of the LaSrCoO$_{4-\delta}$–BZCY cathode under the same condition.

Cathodic overpotential, defined as the deviation from reversible potential as electric current passes through a cathode, is attributed to the slowness of ORR and is an important factor to evaluate cathode performance. It can be calculated with the equation: $\eta_{WE} = \Delta U_{WR} - iR_{el}$, where ΔU_{WR} is the applied voltage between the working and reference electrodes, i is the dc current flowing through the cell and R_{el} is the electrolyte resistance derived from the impedance spectrum. Fig. 7 shows the overpotential of the H-LaSrCoO$_{4-\delta}$–BZCY and the LaSrCoO$_{4-\delta}$–BZCY cathodes as a function of current density at different temperatures. At a given current density, the overpotential of the cathodes decrease with the increase of temperature, reflecting enhanced ORR process at higher temperatures. Meanwhile, the overpotential of the H-LaSrCoO$_{4-\delta}$–BZCY cathode is much lower than that of the LaSrCoO$_{4-\delta}$–BZCY cathode. For instance, the overpotential of the H-LaSrCoO$_{4-\delta}$–BZCY cathode is about 25 mV under a current density of 100 mA cm^{-2} at 750 °C. This value is lower than 70 mV of the LaSrCoO$_{4-\delta}$–BZCY cathode and also much lower than that of some other reported cathodes under the same testing condition [27–29]. Such good performance of the H-LaSrCoO$_{4-\delta}$–BZCY cathode is mainly based on the large amount of oxygen vacancies in the H-LaSrCoO$_{4-\delta}$ lattice, which facilitate the ORR process. Here, the inspection of cathodic overpotential also verifies good properties of H-LaSrCoO$_{4-\delta}$ when used as the cathode material for BZCY based IT-SOFCs. And it is expected that the electrochemical properties of H-LaSrCoO$_{4-\delta}$ will be further improved through changing the Sr doping amount or doping with other transition metals on the B-site [27,30].

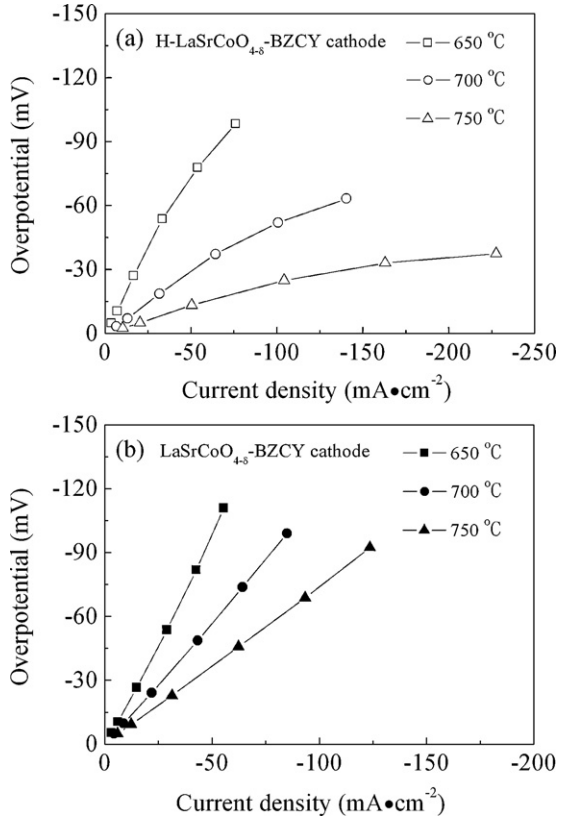

Fig. 7. Overpotential–current density curves of (a) the H-$LaSrCoO_{4-\delta}$–BZCY and (b) the $LaSrCoO_{4-\delta}$–BZCY cathodes.

4. Conclusions

In this study, we synthesized a highly oxygen-deficient phase, H-$LaSrCoO_{4-\delta}$, through solid state reduction of $LaSrCoO_{4-\delta}$ with CaH_2. To evaluate its application in cathodes of BZCY based IT-SOFCs, electrochemical properties of the H-$LaSrCoO_{4-\delta}$–BZCY composite cathode were investigated. At 750 °C, the H-$LaSrCoO_{4-\delta}$–BZCY cathode shows a polarization resistance of 0.229 Ω cm^2. And a cathodic overpotential of 25 mV is obtained under a current density of 100 mA cm^{-2}. Such good properties can be attributed to the large amount of oxygen vacancies in the H-$LaSrCoO_{4-\delta}$ lattice, which enhance the rate-determining steps of dissociation and charge transfer in the cathodic ORR process. It is verified that H-$LaSrCoO_{4-\delta}$ can be used as potential cathode material for BZCY based IT-SOFCs.

Acknowledgement

This project was financially supported by the State Key Laboratory of Electrical Insulation and Power Equipment, Xi'an Jiaotong University.

References

[1] J.P.P. Huijsmans, F.P.F. van Berkel, G.M. Christie, J. Power Sources 71 (1998) 107–110.
[2] C.C. Chao, C.M. Hsu, Y. Cui, F.B. Prinz, ACS Nano 5 (2011) 5692–5696.
[3] R. Chockalingam, S. Chockalingam, V.R.W. Amarakoon, J. Power Sources 196 (2011) 1808–1817.
[4] D. Lee, J.H. Han, Electrochem. Solid State Lett. 14 (2011) B85–B88.
[5] J. Chen, F.L. Liang, L.N. Liu, S.P. Jiang, L. Jian, Int. J. Hydrogen Energy 34 (2009) 6845–6851.
[6] F.L. Liang, J. Chen, S.P. Jiang, B. Chi, J. Pu, L. Jian, Electrochem. Solid State Lett. 11 (2008) B213–B216.
[7] F.L. Liang, J. Chen, S.P. Jiang, B. Chi, J. Pu, L. Jian, Electrochem. Commun. 11 (2009) 1048–1051.
[8] J. Chen, F.L. Liang, B. Chi, J. Pu, S.P. Jiang, L. Jian, J. Power Sources 194 (2009) 275–280.
[9] C.D. Zuo, S.W. Zha, M.L. Liu, M. Hatano, M. Uchiyama, Adv. Mater. 18 (2006) 3318–3320.
[10] C. Jin, J. Liu, Y.H. Zhang, J. Sui, W.M. Guo, J. Power Sources 182 (2008) 482–488.
[11] Y.S. Wang, H.W. Nie, S.R. Wang, T.L. Wen, U. Guth, V. Valshook, Mater. Lett. 60 (2006) 1174–1178.
[12] M. Al Daroukh, V.V. Vashook, H. Ullmann, F. Tietzb, I. Arual Raj, Solid State Ionics 158 (2003) 141–150.
[13] W. Zhou, B.M. An, R. Ran, Z.P. Shao, J. Electrochem. Soc. 156 (2009) B884–B890.
[14] K.T. Lee, A. Manthiram, J. Electrochem. Soc. 153 (2006) A794–A798.
[15] M.A. Hayward, M.J. Rosseinsky, Chem. Mater. 12 (2000) 2182–2195.
[16] H.J. Kitchen, I. Saratovsky, M.A. Hayward, Dalton Trans. 39 (2010) 6098–6105.
[17] M.A. Hayward, M.A. Green, M.J. Rosseinsky, J. Sloan, J. Am. Chem. Soc. 121 (1999) 8843–8854.
[18] K.Q. Huang, J.B. Goodenough, J. Solid State Chem. 136 (1998) 274–283.
[19] A.C. Co, S.J. Xia, V.I. Birss, J. Electrochem. Soc. 152 (2005) A570–A576.
[20] J.E. Sunstrom IV, K.V. Ramanujachary, M. Greenblatt, J. Solid State Chem. 139 (1998) 388–397.
[21] A. Espuirol, N. Brandon, N. Bonanos, J. Kilner, M. Mogensen, B.C.H. Steele, in: A.J. Mc Evoy (Ed.), Proceedings of the Fifth European Solid Oxide Fuel Cell Forum, U. Bossel, Oberrohrdorf, Switzerland (publ.), 2002, p. 225.
[22] J.G. Fisher, D. Rout, K.S. Moon, S.J.L. Kang, Mater. Chem. Phys. 120 (2010) 263–271.
[23] S. Miyoshi, J.O. Hong, K. Yashiro, A. Kaimai, Y. Nigara, K. Kawamura, T. Kawada, J. Mizusaki, Solid State Ionics 161 (2003) 209–217.
[24] T. Ramos, M.D. Carvalho, L.P. Ferreira, M.M. Cruz, M. Godinho, Chem. Mater. 18 (2006) 3860–3865.
[25] X.D. Zhou, Q. Cai, J. Yang, W.B. Yelon, W.J. James, H.U. Anderson, Solid State Ionics 175 (2004) 83–86.
[26] F. Mauvy, J.M. Bassat, E. Boehm, J.P. Manaud, P. Dordor, J.C. Grenier, Solid State Ionics 158 (2003) 17–28.
[27] Q. Li, H. Zhao, L.H. Huo, L.P. Sun, X.L. Cheng, J.C. Grenier, Electrochem. Commun. 9 (2007) 1508–1512.
[28] J.H. Huang, X.Y. Jiang, X.B. Li, A.Q. Liu, J. Electroceram. 23 (2009) 67–71.
[29] Q. Li, Y. Fan, H. Zhao, L.P. Sun, L.H. Huo, J. Power Sources 167 (2007) 64–68.
[30] M. Ferkhi, S. Khelili, L. Zerroual, A. Ringuedé, M. Cassir, Electrochim. Acta 54 (2009) 6341–6346.